# Asymptotic derivation of 2D dynamic equations for FGM plate bending

Julius Kaplunov[1,], Barış Erbaş[1], Nihal Ege[1]

[a] *School of Computing and Mathematics, Keele University, ST5 5BG, UK*
[b] *Department of Mathematics, Eskişehir Technical University, 26470, Eskişehir, Turkey*

**Abstract**

The 3D dynamic equations in elasticity for a thin transversely inhomogeneous plate are subject to asymptotic analysis over the low-frequency range. The leading and first order approximations are derived. The former is given by a biharmonic equation on the mid-plane generalizing the classical Kirchhoff equation for plate bending. A simple explicit formula for the effective bending stiffness is presented. The refined first order equation involves the same biharmonic operator, as the leading order one, along with corrections expressed through Laplacians. However, the constant coefficients at these corrections take the form of sophisticated repeated integrals across the plate thickness. The formulae for the transverse variations of the displacement and stress components, especially relevant for FGM structures, are also obtained. The scope for comparison of the developed asymptotic results and the existing ad hoc considerations on the subject seems to be limited, in contrast to the homogeneous setup, due to a more substantial deviation between the predictions offered by these two approaches.

*Keywords:* thin plate, functionally graded, asymptotic, higher order,

## 1. Introduction

Functionally graded materials (FGM) find various applications in modern technology, in particular, in aerospace [1, 2], automotive [3, 4], defence [5, 6]

*Corresponding author

biomedicine and electronics [7, 8, 9, 10], motivating mathematical modeling of transversely inhomogeneous elastic structures. Numerous publications consider thin functionally graded plates, e.g. see [11, 12, 13, 14, 15, 16, 17, 18, 19, 20]. All the cited papers start from a popular ad hoc approach implementing physical assumptions on stresses and displacements. To the best of our knowledge, more rigorous developments on the subject have not yet been presented. At the same time, analysis of the existing state of art indicates that a number of fundamental issues do not seem to be fully addressed.

First of all, a general 2D equation for plate bending still needs to be properly derived, including a key formula for bending stiffness generalizing the classical one in homogeneous, isotropic set-up. At the same time, many of the papers on the subject, see, for example, [21, 22, 23, 24], operate with rather cumbersome coupled equations combining bending and stretching motions. In particular, [25] unnecessarily suggests to determine a special neutral plane inside the plate for the uncoupling of bending and stretching. Another important problem is concerned with the evaluation of the cross thickness variations of displacements and stresses. It is particularly relevant namely to functionally graded plates for which these variations may take highly nontrivial forms, in contrast to their homogeneous counterparts supporting simple polynomial variations. In addition, the advantages of ad hoc refined theories, e.g. various shear deformation models, appear to be even less obvious than in the homogeneous set-up from the mathematical point of view, e.g. see comparative analysis in [26] and also [27, 28]. Finally, the aforementioned publications dealing with functionally graded plates do not make a further effort to justify the adapted assumptions using more consistent arguments, as well as to present convincing comparisons with 3D benchmark solutions.

At the same time, 2D models for thin homogeneous structures are being derived from the associated 3D equations of elasticity, using mathematically consistent asymptotic methodologies, since long ago. Initially, the asymptotic approach was established for static plate bending deformation [29, 30, 31, 32]. Later on, the asypmtotic approach was extended to a broad range of boundary value problems in mechanics of plates and shells taking into account dynamic phenomena along with a number of other effects, e.g. see research monographs [33, 34, 35, 36, 37, 38] and references therein.

In particular, for a plate, 2D shortened forms of the original 3D dynamic equations have been derived in [26]. It is demonstrated that the leading order approximation is identical to the classical Kirchhoff theory for plate bending. It is remarkable that the higher order approximations in this paper are governed by a fourth order biharmonic equation as the Kirchhoff equation. Recently, an asymptotic composite 2D dynamic equation for plate bending has been established in [39]. This equation governs not only longwave motion but also predicts the short-wavelength limit related to the Rayleigh wave propagating along the plate faces.

In this paper, we extend the homogeneous framework in [26, 35] to a thin functionally graded plate characterized by arbitrary variation of the material parameters across the thickness. The consideration starts from the associated 3D dynamic equation assuming that a typical wavelength is much greater than the plate thickness while a typical time scale corresponds to low-frequency bending motion. The latter is taken the same as in the homogeneous case, as well as the scaling of stresses and displacements.

At leading order, we arrive, seemingly for the first time, at a biharmonic equation with an effective bending stiffness and density explicitly expressed in the paper. In contrast to the current state of art, it elucidates that the peculiarity of transverse shear stresses enables the separation of bending motion from the stretching one. First order corrections, although given by sophisticated formulae, are also derived. As for the homogeneous case, they do not change the order of the leading order equation.

As a numerical illustration, a functionally graded plate with the problem parameters taken in the form of a volume fraction, earlier adapted in [40, 41], is considered. Dispersion curves for leading and first order approximations are plotted along with the graphs demonstrating the effect of the first order correction for static sinusoidal loads applied along plate faces.

## 2. Statement of the Problem

Consider a transversely inhomogeneous elastic layer of thickness $2h$ in Cartesian coordinates $-\infty \leq \alpha_1, \alpha_2 \leq \infty$, $-h \leq \alpha_3 \leq h$. The layer is assumed to be subject to transverse loads $P^{\pm}$ at its faces $\alpha_3 = \pm h$. The problem variable parameters, characterizing mechanical properties of the layer, involve Young's modulus $E = E(\alpha_3)$, Poisson's ratio $\nu = \nu(\alpha_3)$ and density $\rho = \rho(\alpha_3)$.

3D equations of motion in linear elasticity in terms of stresses and displacements are presented as

$$\frac{\partial \sigma_{ii}}{\partial \alpha_i} + \frac{\partial \sigma_{ij}}{\partial \alpha_j} + \frac{\partial \sigma_{3i}}{\partial \alpha_3} - \rho \frac{\partial^2 v_i}{\partial t^2} = 0, \quad i \neq j = 1, 2 \tag{1}$$

$$\frac{\partial \sigma_{i3}}{\partial \alpha_i} + \frac{\partial \sigma_{j3}}{\partial \alpha_j} + \frac{\partial \sigma_{33}}{\partial \alpha_3} - \rho \frac{\partial^2 v_3}{\partial t^2} = 0, \tag{2}$$

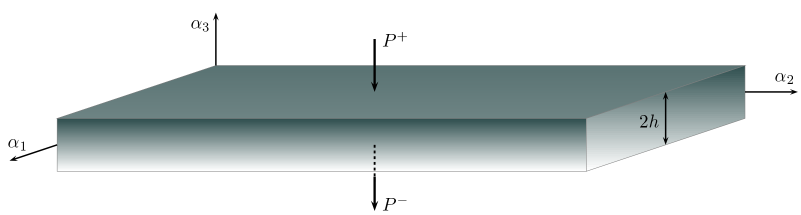


Figure 1: A functionally graded thin plate.

In what follows, stress-displacement relations are taken in the form oriented to asymptotic analysis, e.g. see [26], namely

$$\sigma_{ii} = \frac{E}{1-\nu^2}\left(\frac{\partial v_i}{\partial \alpha_i} + \nu \frac{\partial v_j}{\partial \alpha_j}\right) + \frac{\nu}{1-\nu}\sigma_{33}, \tag{3}$$

$$\sigma_{ij} = \frac{E}{2(1+\nu)}\left(\frac{\partial v_i}{\partial \alpha_j} + \frac{\partial v_j}{\partial \alpha_i}\right), \tag{4}$$

$$\frac{\partial v_3}{\partial \alpha_3} = \frac{1}{E}\left(\sigma_{33} - \nu\left(\sigma_{ii} + \sigma_{jj}\right)\right), \tag{5}$$

$$\frac{\partial v_i}{\partial \alpha_3} = -\frac{\partial v_3}{\partial \alpha_i} + \frac{2(1+\ \nu)}{E}\sigma_{3i}. \tag{6}$$

The boundary conditions at $\alpha_3 = \pm h$ are

$$\sigma_{3i} = 0, \qquad \sigma_{33} = P^{\pm}, \quad \alpha_3 = \pm h. \tag{7}$$

The traditional small geometric parameter in the plate theory is given by

$$\eta = h/L \ll 1, \tag{8}$$

where $L$ is a typical wavelength. In addition, we define a typical time scale

$$T = \frac{L}{\eta c_{20}}, \tag{9}$$

where $c_{20} = \{E_0/2(1+\nu_0)\rho_0\}^{1/2}$ with $E_0 = E(0)$, $\rho_0 = \rho(0)$ and $\nu_0 = \nu(0)$. This scale corresponds to bending vibrations of interest and is taken the same as for homogeneous plates, see [26], also [35].

## 3. Asymptotic Scaling

Let us scale the original spatial and temporal variable according to the setting in the previous section. Consequently,

$$\alpha_i = L\xi_i, \quad \alpha_3 = h\zeta, \quad t = \frac{L}{\eta c_{20}}\tau. \tag{10}$$

The stress and displacement components are nondimensionalized as for homogeneous plate bending (see reference above) using the formulae

$$\begin{aligned} \sigma_{ii} &= E_0\eta\sigma^*_{ii}, & \sigma_{ij} &= E_0\eta\sigma^*_{ij}, \\ \sigma_{3i} &= E_0\eta^2\sigma^*_{3i}, & \sigma_{33} &= E_0\eta^3\sigma^*_{33}, \\ v_i &= L\eta v^*_i, & v_3 &= Lv^*_3. \end{aligned} \tag{11}$$

In what follows, we also set

$$E = E_0E_*, \qquad \rho = \rho_0\rho_*, \quad P^{\pm} = E_0\eta^3P^{\pm}_*. \tag{12}$$

As usual, all the starred quantities above are assumed to be of order unity. Then, equations (1)–(6) and boundary conditions (7) in the previous section, taking into account the relations (10)–(12), can be rewritten in the dimensionless form as

$$\frac{\partial\sigma^*_{3i}}{\partial\zeta} = -\frac{\partial\sigma^*_{ii}}{\partial\xi_i} - \frac{\partial\sigma^*_{ij}}{\partial\xi_j} + \eta^2\frac{\rho_*}{2(1+\nu_0)}\frac{\partial^2 v^*_i}{\partial\tau^2}, \tag{13}$$

$$\frac{\partial\sigma^*_{33}}{\partial\zeta} = -\frac{\partial\sigma^*_{3i}}{\partial\xi_i} - \frac{\partial\sigma^*_{3j}}{\partial\xi_j} + \frac{\rho_*}{2(1+\nu_0)}\frac{\partial^2 v^*_3}{\partial\tau^2}, \tag{14}$$

and

$$\sigma_{ii}^* = \frac{E_*}{1-\nu^2}\left(\frac{\partial v_i^*}{\partial \xi_i} + \nu \frac{\partial v_j^*}{\partial \xi_j}\right) + \eta^2 \frac{\nu}{1-\nu}\sigma_{33}^*, \tag{15}$$

$$\sigma_{ij}^* = \frac{E_*}{2(1+\nu)}\left(\frac{\partial v_i^*}{\partial \xi_j} + \frac{\partial v_j^*}{\partial \xi_i}\right), \tag{16}$$

$$\frac{\partial v_3^*}{\partial \zeta} = -\frac{\eta^2}{E_*}\left(\nu\left(\sigma_{ii}^* + \sigma_{jj}^*\right) - \eta^2 \sigma_{33}^*\right), \tag{17}$$

$$\frac{\partial v_i^*}{\partial \zeta} = -\frac{\partial v_3^*}{\partial \xi_i} + \eta^2 \frac{2(1+\nu)}{E_*}\sigma_{3i}^* \tag{18}$$

with

$$\sigma_{3i}^* = 0, \qquad \sigma_{33}^* = P_*^{\pm}, \quad \text{at} \quad \zeta = \pm 1. \tag{19}$$

The starred stress and displacement components are expanded in an asymptotic series of the form

$$f^* = f^{(0)} + \eta^2 f^{(1)} + \eta^4 f^{(2)} + \cdots \tag{20}$$

resulting in shortened forms of the original 3D equations of various order of accuracy.

## 4. Leading order approximation

Consider the leading order approximation of the problem formulated in the previous section keeping only the terms with the suffix (0) in the asymptotic series (20). First, integrating (17) and (18) along the thickness, we have, respectively,

$$v_3^{(0)} = V_3^{(0)}(\xi,\tau) \quad \text{and} \quad v_i^{(0)} = -\zeta \frac{\partial V_3^{(0)}}{\partial \xi_i} + V_i^{(0)}(\xi,\tau). \tag{21}$$

The last term in (21) is typical for functionally graded plates due to lack of symmetry across the midplane. For homogeneous plates, such term does not appear due to separation of bending and extension deformations, see [35].

Next, inserting displacements (21) into equations (15) and (16), we obtain at leading order

$$\sigma_{ii}^{(0)} = -\frac{E_*}{1-\nu^2}\left[\zeta\left(\frac{\partial^2 V_3^{(0)}}{\partial \xi_i^2} + \nu \frac{\partial^2 V_3^{(0)}}{\partial \xi_j^2}\right) - \left(\frac{\partial V_i^{(0)}}{\partial \xi_i} + \nu \frac{\partial V_j^{(0)}}{\partial \xi_j}\right)\right], \tag{22}$$

and

$$\sigma_{ij}^{(0)} = -\frac{E_*}{1+\nu}\left[\zeta\frac{\partial^2 V_3^{(0)}}{\partial\xi_i\xi_j} - \frac{1}{2}\left(\frac{\partial V_i^{(0)}}{\partial\xi_j} + \frac{\partial V_j^{(0)}}{\partial\xi_i}\right)\right]. \tag{23}$$

Prior to the next round of transformation, it is useful to specify the vector notations

$$\boldsymbol{\sigma}_{sh}^{(k)} = \left(\sigma_{31}^{(k)}, \sigma_{32}^{(k)}\right), \quad \boldsymbol{V}^{(k)} = \left(V_1^{(k)}, V_2^{(k)}\right), \quad k = 0, 1, \ldots \tag{24}$$

and also define the in-plane leading order rotation angle by

$$\theta^{(0)} = \frac{1}{2}\left(\frac{\partial V_1^{(0)}}{\partial\xi_2} - \frac{\partial V_2^{(0)}}{\partial\xi_1}\right). \tag{25}$$

As a result, we deduce from equation (13)

$$\frac{\partial\boldsymbol{\sigma}_{sh}^{(0)}}{\partial\zeta} = \frac{E_*}{1-\nu^2}\left(\zeta\,\mathrm{grad}_2\,\Delta_2 V_3^{(0)} + \nu\,\mathrm{curl}_2(\theta^{(0)}) - \right.$$
$$\left. -\frac{1}{2}\left(\Delta_2\boldsymbol{V}^{(0)} + \mathrm{grad}_2\,\mathrm{div}_2\,\boldsymbol{V}^{(0)}\right)\right) \tag{26}$$

where $\mathrm{curl}_2(\cdot) = (\partial(\cdot)/\partial\xi_2, -\partial(\cdot)/\partial\xi_1)$ and other operators are natural 2D counterparts of the conventional 3D ones.

Now, integrating (26) across the thickness and satisfying the boundary conditions $(19)_1$ we have

$$e_{10}^*\left(\Delta_2\boldsymbol{V}^{(0)} + \mathrm{grad}_2\,\mathrm{div}_2\,\boldsymbol{V}^{(0)}\right) - 2e_{20}^*\,\mathrm{curl}_2\,\theta^{(0)} = 2e_{11}^*\,\mathrm{grad}_2\,\Delta_2 V_3^{(0)} \tag{27}$$

where the constant coefficients $e_{mn}^*$ are defined as

$$e_{mn}^* = e_{mn}/E_0 = \int_{-1}^{1}\frac{s^n\nu^{m-1}(s)E_*(s)}{1-\nu^2(s)}\,ds, \quad n = 0, 1, 2\ldots, \ m = 1, 2. \tag{28}$$

The last equation is the solvability condition for 1D boundary value problem (26) and $(19)_1$. Taking the $\mathrm{div}_2$ of (27) and keeping in mind that $\mathrm{div}_2\,\mathrm{curl}_2 \equiv 0$, we arrive at a simpler formula

$$\mathrm{div}_2\,\boldsymbol{V}^{(0)} = \frac{e_{11}^*}{e_{10}^*}\Delta_2 V_3^{(0)}. \tag{29}$$

Then, we have from (26) and the homogeneous boundary conditions (19) subject to (29)

$$\boldsymbol{\sigma}_{sh}^{(0)} = \left( \frac{e_{11}^*}{e_{10}^*} \mathcal{E}_{10}^*(\zeta) - \mathcal{E}_{11}^*(\zeta) \right) \operatorname{grad}_2 \Delta_2 V_3^{(0)} + \frac{1}{2} \left( \frac{e_{20}^*}{e_{10}^*} \mathcal{E}_{10}^*(\zeta) - \mathcal{E}_{20}^*(\zeta) \right) \operatorname{curl}_2 \theta^{(0)}. \tag{30}$$

where

$$\mathcal{E}_{mn}^*(\zeta) = \mathcal{E}_{mn}(\zeta)/E_0 = \int_\zeta^1 \frac{s^n \nu^{m-1}(s) E(s)}{1-\nu^2(s)}\, ds, \quad n = 0, 1, 2 \ldots, \ m = 1, 2 \tag{31}$$

Finally, the solvability of the problem (14) and $(19)_2$ is written as

$$\int_{-1}^1 \operatorname{div}_2 \boldsymbol{\sigma}_{sh}^{(0)}\, ds - \frac{m_0^*}{2(1+\nu_0)} \frac{\partial^2 V_3^{(0)}}{\partial \tau^2} = P_*^- - P_*^+ \tag{32}$$

where

$$m_n^* = m_n/\rho_0 = \int_{-1}^1 s^n \rho_*(s)\, ds, \quad n = 0, 1, \ldots \tag{33}$$

Expressing from (30) the left hand side of (32), and again benefiting from the identity $\operatorname{div}_2 \operatorname{curl}_2 \equiv 0$, we arrive at the sought for plate bending equation remarkably separated from the effect of extensional deformation. It is

$$\mathcal{D}_* \Delta_2^2 V_3^{(0)} + \frac{m_0^*}{2(1+\nu_0)} \frac{\partial^2 V_3^{(0)}}{\partial \tau^2} = P_*^+ - P_*^- \tag{34}$$

where

$$\mathcal{D}_* = \frac{e_{10}^* e_{12}^* - {e_{11}^*}^2}{e_{10}^*} > 0. \tag{35}$$

Below, we discuss in greater detail the derived equation. Now, for completeness, we also present the formula for $\sigma_{33}^{(0)}$ coming from equations (14), boundary conditions $(19)_2$. It is

$$\sigma_{33}^{(0)} = \left( \frac{e_{11}^*}{e_{10}^*} \int_\zeta^1 \mathcal{E}_{10}^*(s)\, ds - \int_\zeta^1 \mathcal{E}_{11}^*(s)\, ds \right) \Delta_2^2 V_3^{(0)} - \frac{\mathcal{M}_0^*(\zeta)}{2(1+\nu_0)} \frac{\partial^2 V_3^{(0)}}{\partial \tau^2} + P_*^+. \tag{36}$$

where

$$\mathcal{M}_n^*(\zeta) = \mathcal{M}_n(\zeta)/\rho_0 = \int\limits_{\zeta}^{1} s^n \rho(s)\, ds, \quad n = 0, 1, \dots. \tag{37}$$

It is obvious that the last formula satisfies the boundary condition $(19)_2$ at $\zeta = -1$ as well due to (32).

## 5. First order approximation

We now proceed to the next order starting with equation (17). Taking into account (22), we obtain

$$v_3^{(1)} = \mathcal{N}_1(\zeta)\Delta_2 V_3^{(0)} - \mathcal{N}_0(\zeta)\,\mathrm{div}_2\, \boldsymbol{V}^{(0)} + V_3^{(1)}, \tag{38}$$

where the function $\mathcal{N}_n(\zeta)$ is given by the formula (65) in the appendix.

Then, we have from (18)

$$\begin{aligned}\boldsymbol{v}^{(1)} = \mathrm{grad}_2 \left( \mathcal{F}_1^*(\zeta)\Delta_2 V_3^{(0)} + \int\limits_0^{\zeta} \mathcal{N}_0(s)\, ds\, \mathrm{div}_2\, \boldsymbol{V}^{(0)} - \zeta V_3^{(1)} \right) \\ + \mathcal{F}_2^*(\zeta)\,\mathrm{curl}_2(\theta^{(0)}) + \boldsymbol{V}^{(1)}\end{aligned} \tag{39}$$

where $\boldsymbol{v}^{(1)} = (V_1^{(1)}, V_2^{(1)})$ and the function $\mathcal{F}_1^*(\zeta)$ is given by (66) in the appendix, whereas

$$\mathcal{F}_2^*(\zeta) = \int\limits_0^{\zeta} \frac{2(1+\nu(s))}{E_*(s)} \left( \frac{e_{20}^*}{e_{10}^*} \mathcal{E}_{10}^*(s) - \mathcal{E}_{20}^*(s) \right) ds. \tag{40}$$

Next, we obtain from (15) and (16)

$$\begin{aligned}\sigma_{ij}^{(1)} = & \frac{E_*}{1+\nu} \left[ \mathcal{F}_1^*(\zeta) \frac{\partial^2 \Delta_2 V_3^{(0)}}{\partial \xi_i \partial \xi_j} - \zeta \frac{\partial^2 V_3^{(1)}}{\partial \xi_i \partial \xi_j} + \frac{(-1)^i\ \mathcal{F}_2^*(\zeta)}{2} \left( \frac{\partial^2 \theta^{(0)}}{\partial \xi_i^2} - \frac{\partial^2 \theta^{(0)}}{\partial \xi_j^2} \right) \right. \\ & \left. + \int\limits_0^{\zeta} \mathcal{N}_0(s)\, ds \frac{\partial^2\, \mathrm{div}_2\, \boldsymbol{V}^{(0)}}{\partial \xi_i \partial \xi_j} + \frac{1}{2} \left( \frac{\partial V_i^{(1)}}{\partial \xi_j} + \frac{\partial V_j^{(1)}}{\partial \xi_i} \right) \right]\end{aligned} \tag{41}$$

and

$$\sigma_{ii}^{(1)} = \frac{E_*}{1-\nu^2}\left[\left(\mathcal{F}_1^*(\zeta) + \frac{e_{11}^*}{e_{10}^*}\int_0^\zeta \mathcal{N}_0(s)\,ds\right)\Delta_2^2 V_3^{(0)} - \zeta\left(\frac{\partial^2 V_3^{(1)}}{\partial \xi_i^2} + \nu\frac{\partial^2 V_3^{(1)}}{\partial \xi_j^2}\right) + \left(\frac{\partial V_i^{(1)}}{\partial \xi_i} + \nu\frac{\partial V_j^{(1)}}{\partial \xi_j}\right)\right]$$
$$- \frac{E_*}{1+\nu}\left(\mathcal{F}_1^*(\zeta)\frac{\partial^2 \Delta_2 V_3^{(0)}}{\partial \xi_j^2} + (-1)^{i+1}\mathcal{F}_2^*(\zeta)\frac{\partial^2 \theta^{(0)}}{\partial \xi_i \partial \xi_j} + \int_0^\zeta \mathcal{N}_0(s)\,ds\frac{\partial^2\,\mathrm{div}_2\,\boldsymbol{V}^{(0)}}{\partial \xi_j^2}\right)$$
$$+ \frac{\nu}{1-\nu}\left[\left(\frac{e_{11}^*}{e_{10}^*}\int_\zeta^1 \mathcal{E}_{10}^*(s)\,ds - \int_\zeta^1 \mathcal{E}_{11}^*(s)\,ds\right)\Delta_2^2 V_3^{(0)} - \frac{1}{2(1+\nu_0)}\mathcal{M}_0^*(\zeta)\frac{\partial^2 V_3^{(0)}}{\partial \tau^2} + P_*^+\right]. \tag{42}$$

The derivation of (41) and (42) relies on the relation (29).

The solvability of the boundary value problem involving equation (13) and the boundary conditions $(19)_1$ becomes at the first order

$$\int_{-1}^1\left(\frac{\partial \sigma_{ii}^{(1)}}{\partial \xi_i} + \frac{\partial \sigma_{ij}^{(1)}}{\partial \xi_j}\right)ds - \frac{1}{2(1+\nu_0)}\frac{\partial^2}{\partial \tau^2}\left(m_0^* V_i^{(0)} - m_1^*\frac{\partial V_3^{(0)}}{\partial \xi_i}\right) = 0. \tag{43}$$

Now, inserting (41) and (42) into the latter, we arrive at

$$\mathrm{grad}_2\left[\int_{-1}^1 \mathcal{G}^*(s)\,ds\;\Delta_2^2 V_3^{(0)} - e_{11}^*\Delta_2 V_3^{(1)} + \frac{e_{10}^*}{2}\,\mathrm{div}_2\,\boldsymbol{V}^{(1)}\right.$$
$$- \frac{1}{2(1+\nu_0)}\left(\int_{-1}^1 \frac{\nu(s)}{1-\nu(s)}\mathcal{M}_0^*(s)\,ds - m_1^*\right)\frac{\partial^2 V_3^{(0)}}{\partial \tau^2}$$
$$\left. + \int_{-1}^1 \frac{\nu(s)}{1-\nu(s)}\,ds\;P_*^+\right] + \frac{e_{10}^*}{2}\Delta_2 \boldsymbol{V}^{(1)} - e_{20}^*\,\mathrm{curl}_2\,\theta^{(0)}$$
$$+ \frac{1}{2}\Delta_2\,\mathrm{curl}_2\,\theta^{(0)}\int_{-1}^1 \frac{E_*(s)}{1+\nu(s)}\mathcal{F}_2^*(s)\,ds - \frac{m_0^*}{2(1+\nu_0)}\frac{\partial^2 \boldsymbol{V}^{(0)}}{\partial \tau^2} = 0 \tag{44}$$

with the function $\mathcal{G}^*(\zeta)$ given by (64). Consequently,

$$\boldsymbol{\sigma}_{sh}^{(1)} = \int\limits_{\zeta}^{1} \mathcal{G}^*(s)\,ds\;\Delta_2^2\,\mathrm{grad}_2\,V_3^{(0)} - \mathcal{E}_{11}^*(\zeta)\Delta_2\,\mathrm{grad}_2\,V_3^{(1)} +$$
$$+\frac{1}{2}\int\limits_{\zeta}^{1}\frac{E_*(s)}{1+\nu(s)}\mathcal{F}_2^*(s)\,ds\;\Delta_2\,\mathrm{curl}_2\,\theta^{(0)}+$$
$$+\frac{\mathcal{E}_{10}^*(\zeta)}{2}\left(\Delta_2\boldsymbol{V}^{(1)}+\mathrm{grad}_2\,\mathrm{div}_2\,\boldsymbol{V}^{(1)}\right)-\mathcal{E}_{20}^*(\zeta)\,\mathrm{curl}_2\,\theta^{(0)}-$$
$$-\frac{1}{2(1+\nu_0)}\left(\int\limits_{\zeta}^{1}\frac{\nu(s)}{1-\nu(s)}\mathcal{M}_0^*(s)\,ds-\mathcal{M}_1^*(\zeta)\right)\mathrm{grad}_2\,\frac{\partial^2 V_3^{(0)}}{\partial\tau^2}-$$
$$-\frac{\mathcal{M}_0^*(\zeta)}{2(1+\nu_0)}\frac{\partial^2\boldsymbol{V}^{(0)}}{\partial\tau^2}+\int\limits_{\zeta}^{1}\frac{\nu(s)}{1-\nu(s)}\,ds\,\mathrm{grad}_2\,P_*^+. \tag{45}$$

Finally, equation (14) with homogeneous boundary condition $(19)_2$ is solvable at first order provided that

$$\int\limits_{-1}^{1}\mathrm{div}_2\,\boldsymbol{\sigma}_{sh}^{(1)}\,ds-\frac{1}{2(1+\nu_0)}\int\limits_{-1}^{1}\rho_*\,ds\frac{\partial^2 v_3^{(1)}}{\partial\tau^2}=0. \tag{46}$$

Expressing here $\boldsymbol{\sigma}_{sh}^{(1)}$ through (45) and $v_3^{(1)}$ by (38) we obtain

$$\int\limits_{-1}^{1}\left(s-\frac{e_{11}^*}{e_{10}^*}\right)\mathcal{G}^*(s)\,ds\;\Delta_2^3V_3^{(0)}-\mathcal{D}_*\Delta_2^2V_3^{(1)}+$$
$$+\frac{1}{2(1+\nu_0)}\left[\frac{e_{11}^*}{e_{10}^*}\left(\int\limits_{-1}^{1}\frac{\nu(s)}{1-\nu(s)}\mathcal{M}_0^*(s)\,ds+\int\limits_{-1}^{1}\rho_*(s)\mathcal{N}_0(s)\,ds+\right.\right.$$
$$\left.\left.+\frac{e_{11}^*}{e_{10}^*}m_0^*-2m_1^*\right)-\int\limits_{-1}^{1}\frac{s\nu(s)}{1-\nu(s)}\mathcal{M}_0^*(s)\,ds-\int\limits_{-1}^{1}\rho_*(s)\mathcal{N}_1(s)\,ds+m_2^*\right]\frac{\partial^2\Delta_2V_3^{(0)}}{\partial\tau^2}$$
$$-\frac{m_0^*}{2(1+\nu_0)}\frac{\partial^2V_3^{(1)}}{\partial\tau^2}+\int\limits_{-1}^{1}\left(s-\frac{e_{11}^*}{e_{10}^*}\right)\frac{\nu(s)}{1-\nu(s)}\,ds\;\Delta_2P_*^+=0. \tag{47}$$

Let us derive 2D equation along the mid-surface ($\zeta=0$) denoting $w^*=V_3^{(0)}+\eta^2V_3^{(1)}$. To this end, first express $\Delta_2^2V_3^{(0)}$ in (47) from (34) as

$$\Delta_2^2V_3^{(0)}=-\frac{m_0^*}{2\mathcal{D}_*(1+\nu_0)}\frac{\partial^2V_3^{(0)}}{\partial\tau^2}+\frac{1}{\mathcal{D}_*}\left(P_*^+-P_*^-\right) \tag{48}$$

and then add equations (34) and (47) to get within the truncation error $\mathcal{O}(\eta^4)$

$$\mathcal{D}_* \Delta_2^2 w^* + \frac{m_0^*}{2(1+\nu_0)} \left(1 + \eta^2 \mathfrak{a}_* \Delta_2\right) \frac{\partial^2 w^*}{\partial \tau^2} = \left(1 + \eta^2 \mathfrak{b}_*^+ \Delta_2\right) P_*^+ - \left(1 + \eta^2 \mathfrak{b}_*^- \Delta_2\right) P_*^- \tag{49}$$

where the constant coefficients $\mathfrak{a}_*$, $\mathfrak{b}_*^+$ and $\mathfrak{b}_*^-$ are defined in appendix by (63) and (67), respectively.

## 6. 2D equations of motion

Let us write down the 2D derived equations in the previous two sections in dimensional form. In particular, the leading order biharmonic equation (34) becomes

$$\mathcal{D} \Delta_2^2 w + h m_0 \frac{\partial^2 w}{\partial t^2} = P^+ - P^- \tag{50}$$

where $w = L V_3^{(0)}$, $m_0$ is given by (33) and

$$\mathcal{D} = E_0 h^3 \mathcal{D}_* = h^3 \frac{e_{10} e_{12} - e_{11}^2}{e_{10}} \tag{51}$$

with $e_{mn}$ defined by (28). Here and below all operators will be understood in dimensional form, e.g. $\Delta_2 = \partial^2/\partial\alpha_1^2 + \partial^2/\partial\alpha_2^2$.

Equation (50) is a natural extension of that in the classical Kirchhoff theory for thin homogeneous plates. For the latter, we have from the appendix

$$\mathcal{D} = \frac{2 E_0 h^3}{3(1-\nu_0^2)}, \quad m_0 = 2\rho_0 \tag{52}$$

as might be expected.

To the best of our knowledge, the existing publications on the subject, e.g., see, [21, 22, 23, 24], usually operate with coupled equations combining bending and extensional deformation. Seemingly, biharmonic equation (50) with the stiffness given by the general formula (51) has not earlier been suggested.

At next order, we have from (49)

$$\mathcal{D} \Delta_2^2 w + h m_0 \left(1 + h^2 \mathfrak{a}\, \Delta_2\right) \frac{\partial^2 w}{\partial t^2} = \left(1 + h^2 \mathfrak{b}^+ \Delta_2\right) P^+ - \left(1 + h^2 \mathfrak{b}^- \Delta_2\right) P^- \tag{53}$$

where $w = L(V_3^{(0)} + \eta^2 V_3^{(1)})$ and the constant coefficients $\mathfrak{a}$, $\mathfrak{b}^+$ and $\mathfrak{b}^-$ are given in the appendix. In case of a homogeneous plate, $\mathcal{D}$ and $m_0$ are given by (52) as above and

$$\mathfrak{a} = \frac{7\nu_0 - 17}{15(1-\nu_0)}, \quad \mathfrak{b}^+ = \mathfrak{b}^- = -\frac{8 - 3\nu_0}{10(1-\nu_0)} \tag{54}$$

leading to the equation

$$\frac{2E_0 h^3}{3(1-\nu_0^2)}\Delta_2^2 w + 2\rho_0 h \left[1 + h^2 \frac{7\nu_0 - 17}{15(1-\nu_0)}\Delta_2\right]\frac{\partial^2 w}{\partial t^2} = \left[1 - h^2 \frac{8 - 3\nu_0}{10(1-\nu_0)}\Delta_2\right](P^+ - P^-), \tag{55}$$

which is identical to that earlier derived refined plate equation taking into account transverse shear deformation, rotation inertia along with other corrections of the same asypmtotic order, e.g., see, [26, 35]. In the general case, the correction coefficients $\mathfrak{a}$, $\mathfrak{b}^+$ and $\mathfrak{b}^-$ take a sophisticated form and hardly can be derived relying just on physical assumptions, e.g., see, [21], outside the scope of a consistent asymptotic setup.

The advantage of the proposed approach is not restricted to the derivation of the 2D asymptotically consistent equations along the plate mid-surface. In addition, nontrivial explicit formula for through thickness variations of displacement and stress components are established in sections 4 and 5. They are of particular importance in functionally graded structures for which simple polynomial variations, typical for homogeneous plates, are not justified.

## 7. Examples

Consider a functionally graded plate for which

$$E = (E_1 - E_2)\left(\frac{\zeta + 1}{2}\right)^p + E_2, \tag{56}$$

$$\nu = (\nu_1 - \nu_2)\left(\frac{\zeta + 1}{2}\right)^p + \nu_2, \tag{57}$$

and

$$\rho = (\rho_1 - \rho_2)\left(\frac{\zeta + 1}{2}\right)^p + \rho_2, \tag{58}$$

with the material properties of the plate varying from Nickel at the lower surface $\zeta = -1$ with $E_2 = 223.95 \times 10^9$ N/m$^2$, $\nu_2 = 0.31$ and $\rho_2 = 8900$ kg/m$^3$ to stainless steel at the upper surface $\zeta = 1$ with $E_1 = 201.04 \times 10^9$ N/m$^2$, $\nu_1 = 0.3262$ and $\rho_1 = 8166$ kg/m$^3$, e.g., see, [40], also [41]. In this case, we have for the coefficients in equations (50) and (53)

Table 1: The values of the coefficients appearing in (53) for $h = 0.01$m.

| | $p = 1$ | $p = 5$ | $p = 15$ |
|---|---|---|---|
| $\mathcal{D}$ | 157471 | 160786 | 162916 |
| $m_0$ | 17066 | 17555.3 | 17708.3 |
| $\mathfrak{a}$ | $-1.44329$ | $-1.41269$ | $-1.41915$ |
| $\mathfrak{b}^+$ | $-1.01872$ | $-0.99460$ | $-1.00651$ |
| $\mathfrak{b}^-$ | $-1.04532$ | $-1.01291$ | $-1.0149$ |

Below, we plot the dispersion curves corresponding to the solutions of equations (50) and (53) taken in the form $w = \exp(i(k\alpha_1 - \omega t))$ where $\omega$ is circular frequency and $k$ is wavenumber. They are given, respectively, by

$$K = \left(\frac{m_0 h^3 E_2}{\mathcal{D}\rho_2}\right)^{1/4} \sqrt{\Omega} \tag{59}$$

and

$$K = \left(\sqrt{\frac{\mathcal{D}\rho_2}{m_0 h^3 E_2} + \left(\frac{\mathfrak{a}\Omega}{2}\right)^2} - \frac{\mathfrak{a}\Omega}{2}\right)^{1/2} \sqrt{\frac{m_0 h^3 E_2}{\mathcal{D}\rho_2}\Omega} \tag{60}$$

In Figure 2, we specify the dimensionless parameters $K = kh$ and $\Omega = \omega h\sqrt{\rho_2/E_2}$ setting $\nu_1 = 0.31$ and $\nu_2 = 0.3262$ .

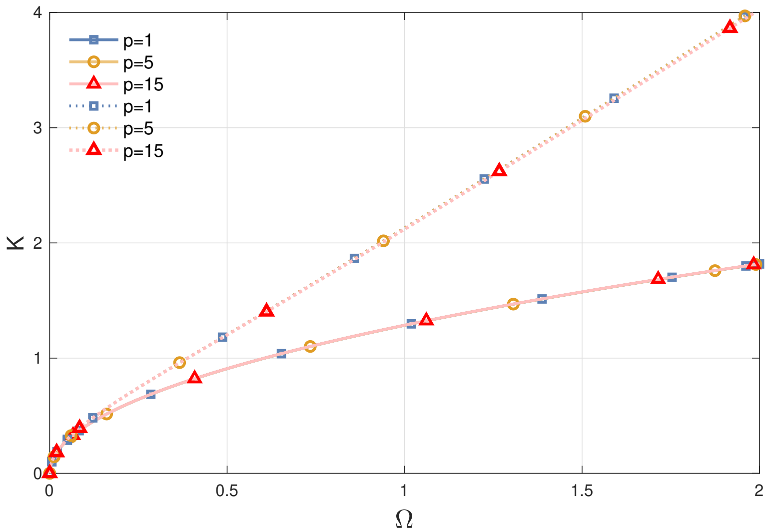


Figure 2: Dispersion curves corresponding to (59) and (60) corresponding to FG plate characterized by (56)–(58) for various values of volume fraction exponent $p$.

We also look at the solution of the static problem for which $P^+ = -P^- = \mathcal{D}\delta^4 h^{-4}\cos(\delta\alpha_1/h)/2$. In this case, equations (50) and (53) result in the normalized displacement amplitude given, respectively, by

$$w = w_1 = 1 \tag{61}$$

and

$$w = w_2 = 1 - \frac{\delta^2}{2}(\mathfrak{b}^+ - \mathfrak{b}^-). \tag{62}$$

In Figure 3, the relative error $r = |(w_2 - w_1)/w_1| \times 100\% = \delta^2|\mathfrak{b}^+ - \mathfrak{b}^-| \times 50\%$ is plotted versus the dimensionless parameter $\delta$.

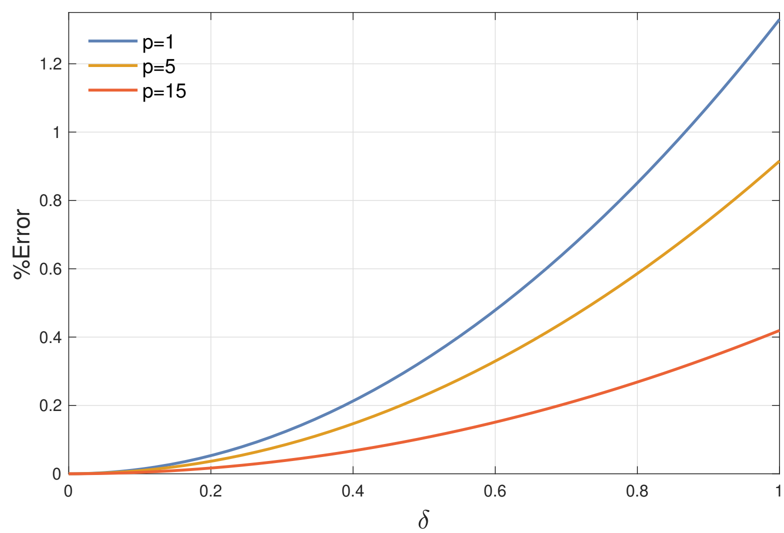


Figure 3: Relative error between the leading and refined normalized displacement amplitudes (61) and (62).

## 8. Conclusion

The asymptotic technique developed in the paper naturally generalizes previous considerations for homogeneous plates, e.g. see [26, 35]. The established framework is also similar to the conventional homogenisation procedure for periodic media adapted for thin layers, e.g. see [42, 43], and also [44] dealing with an inhomogeneous viscoelastic bar and the most recent consideration in [45] concerned with a plane strain problem for a thin-walled functionally graded cylinder.

The leading order approximation of the original 3D equations of motion is given by biharmonic plate bending equation (34) on the mid-plane. It is shown that the separation of the bending motion of interest from the stretching one is due to the decomposition of the transverse shear stress vector into irrotational and solenoidal components, see (30). This fact has not been noted in the earlier publications, see [21, 22, 23, 24, 25, 40, 41].

The refined equation for plate bending (49) contains first order corrections given by lengthy formulae presented in the appendix. They can hardly be derived outside the proposed asymptotic scheme, relying just on an intuitive physical insight. This observation is also true for intricate formulae in sections 4 and 5 expressing the variations of the displacement and stress components.

The implementation of the obtained results is not restricted to a typical FGM plate considered in section 7. In particular, they can readily be adapted for the asymptotic justification and refinement of many of the existing laminated plate models, e.g. see the substantial monograph [46], of course, with the exception of high-contrast laminates [47], for which the assumed scaling above must be altered.

The asymptotic approach works for functionally graded plates and can be extended to functionally graded shells, coatings, and interfaces;

There is little room for ad-hoc considerations on the subject, especially for refined models.

## 9. Appendix

The correction coefficients appearing in equation (53) can be written as

$$\begin{aligned}\mathfrak{a} = \mathfrak{a}_* = \frac{h^3}{\mathcal{D}} \int_{-1}^{1} \left( s - \frac{e_{11}}{e_{10}} \right) \mathcal{G}(s)\, ds - \frac{1}{m_0} \Bigg( \frac{e_{11}}{e_{10}} \Bigg( \int_{-1}^{1} \frac{\nu(s)}{1-\nu(s)} \mathcal{M}_0(s)\, ds \\ + \int_{-1}^{1} \rho(s) \mathcal{N}_0(s)\, ds + \frac{e_{11}}{e_{10}} m_0 - 2 m_1 \Bigg) - \int_{-1}^{1} \frac{s\nu(s)}{1-\nu(s)} \mathcal{M}_0(s)\, ds \\ - \int_{-1}^{1} \rho(s) \mathcal{N}_1(s)\, ds + m_2 \Bigg)\end{aligned} \tag{63}$$

where

$$\mathcal{G}(\zeta) = E_0\mathcal{G}^*(\zeta) = \frac{E(\zeta)}{1-\nu^2(\zeta)}\left(\mathcal{F}_1(\zeta) + \frac{e_{11}}{e_{10}}\int\limits_0^\zeta \mathcal{N}_0(s)\,ds\right) + \frac{\nu(\zeta)}{1-\nu(\zeta)}\int\limits_\zeta^1 \left(\frac{e_{11}}{e_{10}}\mathcal{E}_{10}(s) - \mathcal{E}_{11}(s)\right) ds \tag{64}$$

and

$$\mathcal{N}_n(\zeta) = \int\limits_0^\zeta \frac{s^n\nu(s)}{1-\nu(s)}\,ds, \qquad n = 0, 1, 2, \dots \tag{65}$$

with

$$\mathcal{F}_1(\zeta) = \mathcal{F}_1^*(\zeta) = \int\limits_0^\zeta \frac{2(1+\nu(s))}{E(s)}\left(\frac{e_{11}}{e_{10}}\mathcal{E}_{10}(s) - \mathcal{E}_{11}(s)\right) ds - \int\limits_0^\zeta \mathcal{N}_1(s)\,ds \tag{66}$$

and other quantities above presented in the main body of the paper, whereas

$$\mathfrak{b}^+ = \mathfrak{b}_*^+ = \int\limits_{-1}^1 \left(s - \frac{e_{11}}{e_{10}}\right)\frac{\nu(s)}{1-\nu(s)}\,ds + \frac{h^3}{\mathcal{D}}\int\limits_{-1}^1 \left(s - \frac{e_{11}}{e_{10}}\right)\mathcal{G}(s)\,ds \tag{67}$$

$$\mathfrak{b}^- = \mathfrak{b}_*^- = \frac{h^3}{\mathcal{D}}\int\limits_{-1}^1 \left(s - \frac{e_{11}}{e_{10}}\right)\mathcal{G}(s)\,ds.$$

## References


[1] M. Niino, T. Hirai, R. Watanabe, The functionally gradient materials, J. Jpn. Soc. Compos. Mater 13 (1987) 257–264.

[2] J. Kim, W.-J. Kim, D. Choi, J. Park, W.-S. Ryu, Design of a C/SiC functionally graded coating for the oxidation protection of C/C composites, Carbon 43 (8) (2005) 1749–1757.

[3] G. Udupa, K. Gangadharan, et al., Future applications of carbon nanotube reinforced functionally graded composite materials, in: IEEE-international conference on advances in engineering, science and management (ICAESM-2012), IEEE, 2012, pp. 399–404.

[4] Y. Li, S. Jian, Z. Min, Application of ceramics metal functionally graded materials on green automobiles, in: Key Engineering Materials, Vol. 280, Trans Tech Publ, 2005, p. 1925.

[5] E. S. Chin, Army focused research team on functionally graded armor composites, Materials Science and Engineering: A 259 (2) (1999) 155–161.

[6] N. Gupta, V. Prasad, V. Madhu, B. Basu, Ballistic studies on TiB 2-Ti functionally graded armor ceramics., Defence Science Journal 62 (6) (2012).

[7] W. Pompe, H. Worch, M. Epple, W. Friess, M. Gelinsky, P. Greil, U. Hempel, D. Scharnweber, K. Schulte, Functionally graded materials for biomedical applications, Materials Science and Engineering: A 362 (1-2) (2003) 40–60.

[8] X. Miao, D. Sun, Graded/gradient porous biomaterials, Materials 3 (1) (2010) 26–47.

[9] E. Mueller, Č. Drašar, J. Schilz, W. Kaysser, Functionally graded materials for sensor and energy applications, Materials Science and Engineering: A 362 (1-2) (2003) 17–39.

[10] I. Bharti, N. Gupta, K. Gupta, Novel applications of functionally graded nano, optoelectronic and thermoelectric materials, International Journal of Materials, Mechanics and Manufacturing 1 (3) (2013) 221–224.

[11] H. Altenbach, V. A. Eremeyev, Direct approach-based analysis of plates composed of functionally graded materials, Archive of Applied Mechanics 78 (10) (2008) 775–794.

[12] A. Saidi, E. Jomehzadeh, On the analytical approach for the bending/stretching of linearly elastic functionally graded rectangular plates with two opposite edges simply supported, Proceedings of the Institution of Mechanical Engineers, Part C: Journal of Mechanical Engineering Science 223 (9) (2009) 2009–2016.

[13] A. H. Baferani, A. Saidi, E. Jomehzadeh, Exact analytical solution for free vibration of functionally graded thin annular sector plates resting on elastic foundation, Journal of Vibration and Control 18 (2) (2012) 246–267.

[14] M. Amirpour, R. Das, E. I. S. Flores, Bending analysis of thin functionally graded plate under in-plane stiffness variations, Applied Mathematical Modelling 44 (2017) 481–496.

[15] A. H. Baferani, A. Saidi, H. Ehteshami, On free vibration of functionally graded Mindlin plate and effect of in-plane displacements, Journal of Mechanics 29 (2) (2013) 373–384.

[16] A. Nosier, F. Fallah, Reformulation of Mindlin–Reissner governing equations of functionally graded circular plates, Acta Mechanica 198 (3) (2008) 209–233.

[17] A. Fereidoon, A. Mohyeddin, et al., Bending analysis of thin functionally graded plates using generalized differential quadrature method, Archive of Applied Mechanics 81 (11) (2011) 1523–1539.

[18] A. Damanpack, M. Bodaghi, H. Ghassemi, M. Sayehbani, Boundary element method applied to the bending analysis of thin functionally graded plates, Latin American Journal of Solids and Structures 10 (3) (2013) 549–570.

[19] J. Jedrysiak, Free vibrations of thin functionally graded plates with microstructure, Engineering structures 75 (2014) 99–112.

[20] J. L. Mantari, A. S. Oktem, C. G. Soares, Bending response of functionally graded plates by using a new higher order shear deformation theory, Composite Structures 94 (2) (2012) 714–723.

[21] J. Reddy, Analysis of functionally graded plates, International Journal for numerical methods in engineering 47 (1-3) (2000) 663–684.

[22] A. M. Zenkour, Generalized shear deformation theory for bending analysis of functionally graded plates, Applied Mathematical Modelling 30 (1) (2006) 67–84.

[23] I. Mechab, H. A. Atmane, A. Tounsi, H. A. Belhadj, et al., A two variable refined plate theory for the bending analysis of functionally graded plates, Acta Mechanica Sinica 26 (6) (2010) 941–949.

[24] J. Reddy, E. Ruocco, J. A. Loya, A. M. Neves, Theories and analyses of functionally graded circular plates, Composites Part C: Open Access (2021) 100166.

[25] S. Abrate, Functionally graded plates behave like homogeneous plates, Composites part B: engineering 39 (1) (2008) 151–158.

[26] A. Goldenveizer, J. Kaplunov, E. Nolde, On Timoshenko-Reissner type theories of plates and shells, International Journal of Solids and Structures 30 (5) (1993) 675–694.

[27] J. G. Simmonds, An asymptotic analysis of end effects in the axisymmetric deformation of elastic tubes weak in shear: Higher-order shell theories are inadequate and unnecessary, International Journal of Solids and Structures 29 (20) (1992) 2441–2461.

[28] J. G. Simmonds, Some comments on the status of shell theory at the end of the 20th century-complaints and correctives, in: 38th Structures, Structural Dynamics, and Materials Conference, 1998, p. 1074.

[29] A. Goldenveizer, The approximation of the plate bending theory by the asymptotic analysis of elasticity theory, Pr. Math. Mech 26 (4) (1962) 668–686.

[30] K. Friedrichs, R. Dressler, A boundary-layer theory for elastic plates, Communications on Pure and Applied Mathematics 14 (1) (1961) 1–33.

[31] A. E. Green, On the linear theory of thin elastic shells, Proceedings of the Royal Society of London. Series A. Mathematical and Physical Sciences 266 (1325) (1962) 143–160.

[32] A. L. Goldenveizer, The principles of reducing three-dimensional problems of elasticity to two-dimensional problems of the theory of plates and shells, in: Proceedings, Eleventh International Congress of Theoretical and Applied Mechanics, Springer-Verlag, Berlin, 1964, pp. 306–311.

[33] A. L. Goldenveizer, Theory of thin elastic shells, Izdatelstvo Nauka, In Russian, Moscow, 1976.

[34] P. G. Ciarlet, Plates and junctions in elastic multi-structures: an asymptotic analysis, Vol. 14, Springer Verlag, 1990.

[35] J. Kaplunov, L. Y. Kossovitch, E. Nolde, Dynamics of thin walled elastic bodies, Academic Press, 1998.

[36] K. C. Le, Vibrations of shells and rods, Springer Science & Business Media, 2012.

[37] V. L. Berdichevsky, Variational Principles of Continuum Mechanics. II. Applications, Springer-Verlag, Berlin, 2009.

[38] L. A. Aghalovyan, Asymptotic theory of anisotropic plates and shells, World Scientific, 2015.

[39] B. Erbaş, J. Kaplunov, E. Nolde, M. Palsü, Composite wave models for elastic plates, Proceedings of the Royal Society A: Mathematical, Physical and Engineering Sciences 474 (2214) (2018) 20180103.

[40] C. Loy, K. Lam, J. Reddy, Vibration of functionally graded cylindrical shells, International Journal of Mechanical Sciences 41 (3) (1999) 309–324.

[41] Z. Iqbal, M. N. Naeem, N. Sultana, Vibration characteristics of FGM circular cylindrical shells using wave propagation approach, Acta Mechanica 208 (3) (2009) 237–248.

[42] G. P. Panasenko, Multi-scale modelling for structures and composites, Springer, Dordrecht, 2005.

[43] R. Craster, L. Joseph, J. Kaplunov, Long-wave asymptotic theories: the connection between functionally graded waveguides and periodic media, Wave Motion 51 (4) (2014) 581–588.

[44] J. Kaplunov, A. Shestakova, I. Aleynikov, B. Hopkins, A. Talonov, Low-frequency perturbations of rigid body motions of a viscoelastic inhomogeneous bar, Mechanics of Time-Dependent Materials 19 (2) (2015) 135–151.

[45] N. Ege, B. Erbaş, J. Kaplunov, N. Noori, Low-frequency vibrations of a thin-walled functionally graded cylinder (plane strain problem), Mechanics of Advanced Materials and Structures (2022) 1–9.

[46] J. N. Reddy, Mechanics of laminated composite plates and shells: Theory and Analysis, 2nd Edition, CRC Press, 2003.

[47] J. Kaplunov, D. Prikazchikov, L. Prikazchikova, Dispersion of elastic waves in a strongly inhomogeneous three-layered plate, International Journal of Solids and Structures 113 (2017) 169–179.